Title

Small-Animal Compression Models of Osteoarthritis.

Authors

Chan, Deva

van der Meulen, Marjolein

Maerz, Tristan

et al.

Publication Date

2023

DOI

10.1007/978-1-0716-2839-3_25

Peer reviewed

HHS Public Access

Author manuscript

Methods Mol Biol. Author manuscript; available in PMC 2024 January 01.

Published in final edited form as:

Methods Mol Biol. 2023 ; 2598: 345–356. doi:10.1007/978-1-0716-2839-3_25.

Small-Animal Compression Models of Osteoarthritis

Blaine A. Christiansen[1], **Deva D. Chan**[2], **Marjolein C. H. van der Meulen**[3], **Tristan Maerz**[4]

[1]University of California Davis, Department of Orthopaedic Surgery

[2]Purdue University, Weldon School of Biomedical Engineering

[3]Cornell University, Meinig School of Biomedical Engineering and Sibley School of Mechanical & Aerospace Engineering

[4]University of Michigan, Departments of Orthopaedic Surgery and Biomedical Engineering

Abstract

The utility of nonsurgical, mechanical compression-based joint injury models to study osteoarthritis pathogenesis and treatments is increasing. Joint injury may be induced via cyclic compression loading or acute overloading to induce anterior cruciate ligament rupture. Models utilizing mechanical testing systems are highly repeatable, require little expertise, and result in a predictable onset of osteoarthritis-like pathology on a rapidly progressing timeline. In this chapter, we describe the procedures and equipment needed to perform mechanical compression-induced initiation of osteoarthritis in mice and rats.

Keywords

Osteoarthritis; post-traumatic; animal models; cartilage; anterior cruciate ligament; compression; injury

1. Introduction

Rodent models of osteoarthritis (OA) are essential tools for studying the pathogenesis and treatment of OA on an accelerated timeline (from 10–20 years in humans to 4–12 weeks in rodent models). All animal models of OA initiate cartilage degradation, but many currently used models do not reproduce clinically-relevant injury conditions, due to invasive and non-physiologic injury methods most commonly involving surgery. In addition, these methods often cause an injury response due to invasive surgical procedures, complicating studies of the inflammatory response associated with the injury itself. Due to these limitations, there is emerging interest in compression models of OA that can non-invasively induce joint injury and resultant degeneration in mice and rats. These procedures use externally-applied mechanical loads to overload the articular cartilage and/or injure the anterior cruciate ligament (ACL), more closely mimicking injury conditions relevant to humans. Non-invasive models do not break the skin or disrupt the joint capsule, and

Correspondence: Blaine A. Christiansen, Ph.D., University of California Davis Health, Department of Orthopaedic Surgery, 4635 2nd Ave, Suite 2000, Sacramento, CA 95817, Phone: 916-734-3974, bchristiansen@ucdavis.edu.

are therefore completely aseptic, which avoids potential confounding effects caused by the surgical/invasive injury procedure. Furthermore, in models utilizing mechanical testing systems, injury loading is highly repeatable and less prone to operator variability, potentially affecting disease onset and progression in surgical OA models.

Established non-invasive compression models of OA generally apply controlled loads to the rodent limb, and include the cyclic compression model in mice [1–5], and the overload ACL rupture (ACL-R) model in mice [6–10] and rats [11–15]. These models can be implemented using a variety of methods, each with its own advantages, limitations, and technical considerations (see Notes 1–10). The objectives of this chapter are to discuss the implementation of compression models of OA, including Cyclic Compression in Mice (see Notes 11–19), ACL Rupture in Mice (see Notes 20–33), and Rat ACL Rupture in Rats (see Notes 34–44), and to share best practices to facilitate repeatable injury and disease induction when employing these methods in preclinical studies of OA.

2. Materials

1. Animals – mice or rats. These procedures can be applied for any genetic strain, age, or sex (see Notes 11, 12, 20, and 35)
2. Commercially-available materials testing systems such as the Electroforce 3200 (TA Instruments, New Castle, DE) or equivalent (see Note 6)
3. Load cells for mice require approximately 20 N capacity; load cells for rats require approximately 200 N capacity (see Notes 33 and 44)
4. Appropriately-sized fixtures that restrict medial-lateral motion of the knee and foot (see Note 7)
5. Anesthetic during loading: ketamine/xylazine or, preferably, inhaled isoflurane (2–4%) (see Note 4)
6. Analgesic post-injury for ACL-R models: e.g., 5 mg/kg SC Carprofen and/or 0.05 mg/kg SC buprenorphine

3. Methods

3.1. Mouse Cyclic Compression (see Notes 11–19):

1. Anesthetize mice and ensure adequate anesthesia with toe pinch and/or tail pinch
2. Place the mouse supine, with the lower leg positioned horizontally (parallel to the body) between two loading platens (see Fig. 1)
3. Apply a preload of 0.5–1 N to position the lower leg
4. Apply cyclic loading for the designated number of cycles (see Notes 11–13)
5. Repeat procedures for each daily loading bout for the designated number of days and weeks to induce OA (see Note 13)

3.2. Mouse ACL-R (see Notes 20–33):

1. Anesthetize animals and ensure adequate anesthesia with toe pinch and/or tail pinch
2. Place the mouse prone, with the lower leg positioned vertically (perpendicular to the body) between two loading platens with the hip in full extension (see Fig. 2)
3. Apply a preload of 1–2 N to hold the lower leg in place
4. Apply a single compressive load with a loading rate of 1–10 mm/s to a target force (~12–15 N) or until ACL injury
5. Injury is typically accompanied by an auditory cue (“click” or “crunch”) and force release on the force-displacement plot, after which the load can be manually stopped (see Fig. 2)
6. Alternatively, the ACL can be injured by applying a considerably faster load (~200 mm/s) to a target displacement (1.7 mm) (see Note 21)
7. ACL injury can be confirmed using an anterior drawer test, or with standard radiography (e.g. Faxitron) following injury loading to rule out fractures
8. Provide at least one dose of analgesic post-injury and additional doses as needed

3.3. Rat ACL-R (see Notes 34–44):

1. Anesthetize animals and ensure adequate anesthesia with toe pinch and/or tail pinch
2. Place the rat prone, with the lower leg positioned vertically in the system (see Fig. 3)
3. Apply a 3 N preload for 10 s
4. Optional: apply 10 preconditioning cycles, cycling from 1–5 N at 0.5 Hz. Preconditioning cycles can aid in seating the joint in the fixtures but may not be necessary
5. Apply a preload ramp at 0.1 mm/s from 1–15 N
6. Apply a failure ramp at 8 mm/s to a target displacement of 3 mm
7. Injury is typically accompanied by an auditory cue (“click” or “crunch”) and force release on the force-displacement plot (see Note 35)
8. ACL injury can be confirmed using an anterior drawer test, or with standard radiography (e.g. Faxitron) following injury loading to rule out fractures (see Note 36)
9. Provide at least one dose of analgesic post-injury and additional doses as needed

4. Notes

1. Once successfully set up, these methods are easy to learn with not much expertise required, which likely reduces inter- and intra-user variability compared to surgical or even injection models
2. Injury/loading is highly reproducible (although faster loading rates, i.e. >10 mm/s are somewhat less reproducible), with a predictable pattern of joint degeneration
3. For models utilizing mechanical testing systems, although not necessary, it is generally recommended that two people perform the procedure: one person to operate the mechanical testing system and one person to anesthetize, configure, and monitor the animals
4. Total anesthesia time for inhaled isoflurane, in the absence of other procedures, is typically 5–10 mins, followed by an additional ~5 mins of recovery monitoring after loading. Short procedure time and use of isoflurane for anesthesia enables rapid recovery and minimal anesthesia-dependent effects, and allows these methods to be high throughput
5. Due to being non-invasive and completely aseptic, all of these methods allow for the study of inflammation, ectopic intra-articular bone formation, joint biomechanics, or other processes at early time points, even only a few minutes after injury
6. Implementation typically involves a commercially available materials testing system, but can also be achieved using a custom-built system or a small handheld device and laptop computer. However, these custom systems often have limited capabilities for high velocities and real-time measurement and control of force and displacement
7. These procedures require custom-made fixtures that often vary between research groups. Knee fixtures must be able to hold the lower leg stationary during loading without the knee “slipping out”. A shallow knee cup that does not constrain translation of the tibia will be more likely to result in ACL rupture. A deeper knee cup will allow for higher magnitude loading without acute ACL injury [16]. As an alternative to a cup, a channel/trough may be milled with a ball-end mill (facilitating rounded edges), which restricts medial-lateral motion while allowing for anterior translation of the tibia. Quadriceps tendon injury during loading can be avoided/mitigated with padding and/or rounding of edges on the knee fixture
8. Degree of knee flexion may influence joint damage and likelihood of ACL injury. Tension in the quadriceps during hip extension makes ACL rupture more likely by pulling the tibia anteriorly, while tension in the hamstrings during flexion makes ACL rupture less likely by pulling the tibia posteriorly [16]. For both mouse and rat ACL-R, the knee joint should be in ~90–100° of flexion.

9. The flexion angle of the ankle may also influence likelihood of ACL injury. Greater ankle flexion creates tension in the gastrocnemius and soleus and causes anterior tibial translation, making ACL injury more likely [16]. For both mouse and rat ACL-R procedures, the ankle joint should be in 30° of flexion (see Figs. 2 and 3)

10. Rotation of the lower limb also plays a role in the likelihood of inducing an ACL rupture during tibial compression [12]. Similarly, body and contralateral limb position are important, as pelvic rotation induces ipsilateral femoral internal/external rotation. Elevating the contralateral limb to the height of the loaded limb ensures a neutral pelvic rotation

4.1. Cyclic Compression in Mice:

11. The applied loading waveform and loading rate for mouse cyclic compression are based on osteogenic loading of the metaphysis [17, 18]. A common loading frequency is 4 Hz, corresponding to the walking frequency of the mouse at ~4% strain per second, with a dwell between each load-unload cycle (see Fig. 1c).

12. Load magnitude varies with animal age and strain. Generally, loads are in the 7–10 N range. Altering the load magnitude and number of loading bouts modulates the amount of joint damage generated

13. For mouse cyclic compression, 1,200 cycles are typically applied in each daily loading bout, 5 days per week for multiple weeks, although a single bout of loading produces similar effects to daily loading after 1 and 2 weeks [19]

14. Cyclic compression loading of mice induces compression and shear at the joint through AP translation of the tibia and rotation of the femur [20]

15. Daily in vivo loading induces cartilage damage in both male and female mice; degenerative changes are mouse-strain specific and progress over time [4]

16. Bone mass changes occur in the subchondral, epiphyseal and metaphyseal bone. Over time, daily loading enhances bone mass at the metaphysis. Changes in bone mass closer to the joint surface are more variable and may initially decrease at early time points, followed by increased bone mass with time.

17. Osteophytes/enthesophytes form on the medial aspect of the joint at the MCL insertion. These structures are cartilaginous after 1 and 2 weeks of loading, and are mineralized at 6 weeks of loading

18. Joint fibrosis is present, but not classical inflammation. The degree of fibrosis differs substantially across different mouse strains

19. Gait analysis shows no major differences in loaded animals

4.2. ACL-R in Mice:

20. ACL injury of mice typically occurs between 8–15 N; injury force correlates positively with body mass (but not sex) [10]

21. Using a higher speed loading rate is more likely to induce midsubstance tear of the ACL, rather than avulsion from the distal femur [7]. Real-time monitoring of injury on the force-displacement plot may be more difficult with high-speed loading

22. Following ACL-R in mice, joint degeneration progresses to severe OA by 4–6 weeks; the medial side of the joint is more affected than the lateral side

23. OA in older mice typically progresses slightly faster than in young mice [21]; OA progression is typically similar in male and female mice [22]

24. ACL deficiency causes the articulation of the femur to move to a more posterior position on the proximal tibia; this can lead to dislocation of the posterior horn of the medial meniscus

25. ACL-R results in joint instability, and OA progression may be largely driven by mechanical factors. This model typically can't be adjusted to produce a milder injury or slower PTOA progression

26. Joint inflammation, synovitis, and protease activity are observed primarily during the first 2–3 weeks, peaking around 1–14 days post-injury [23]

27. Considerable synovial fibrosis and chondrophyte formation occur within the first 1–2 weeks; mineralized osteophytes are present by 4 weeks post-injury, which will continue to progressively grow and mineralize [24]

28. Osteophytes are commonly observed on the medial side of the distal femur, the posterior-medial proximal tibia, and the anterior horn of the medial meniscus [24]

29. Epiphyseal trabecular bone loss (~20–30% decrease in BV/TV) occurs during the first 2 weeks post-injury, primarily due to trabecular thinning; this bone loss is partially recovered at later time points

30. Thinning of the subchondral bone plate also occurs during the first 2 weeks post-injury; at later time points, this is reversed and subchondral bone plate thickness is increased in injured joints

31. No significant differences in overall activity level of mice following injury, though gait analysis indicates some gait asymmetry [25]

32. If possible, the mechanical testing system can be programmed to return to the "zero-displacement" position immediately after a sudden drop in load is detected to reduce the joint from the subluxed position

33. It is recommended to program load and displacement limits to avoid overloading or damage to load cells, fixtures, or the mechanical testing system. For mice, a load limit of 20–25 N and a displacement limit of ~2.0 mm is recommended. These are dependent on strain and skeletal size, and careful preliminary testing is recommended to determine these limits.

4.3. ACL-R in Rats:

34. ACL-R creates joint instability, and OA progression may be largely driven by mechanical factors; this model typically can't be adjusted to produce a milder injury or slower PTOA progression

35. For a 200–250 g Lewis rat, the failure load is typically 60 – 70 N, at a displacement of 2.2 – 2.5 mm. Force release associated with ACL rupture may not be easily detectable on force-displacement plot for rat injuries

36. Important: distal femoral physeal dislocations/fractures can give a false-positive anterior drawer test. These are most common in the rat ACL-R model. Cadaveric animals should be used to practice the procedure and confirm ACL injury by dissection to avoid physeal injuries

37. Early articular cartilage damage is observed by 1–2 weeks post-injury, including surface fibrillation and acute necrosis [26]

38. Moderate OA is observed by 4–6 weeks post-injury, and severe OA is observed by 10 weeks

39. Medial compartment damage is more severe than lateral compartment, with up to 2x OARSI grade on the medial femoral condyle compared to the lateral femoral condyle at 4 weeks [27]

40. Synovitis is observed as early as 3 days post-injury, maximal between 3–14 days, and synovial fibrosis persists up to 16 weeks post-injury [14, 28]

41. Osteophyte formation is commonly observed in the medial compartment, notably at the anterior medial condyle, posterior medial tibial plateau, and anterior medial meniscus. In general, osteophytes are larger in mice than in rats relative to the size of the joint

42. Acute epiphyseal trabecular bone loss (~20–30% decrease in BV/TV) and subchondral bone thinning (~15–20%) is observed within the first 2 weeks. Persistent bone volume deficit of 5–10% is observable for at least 10 weeks post-injury [26, 29]. Bone loss has been associated with both reduced bone formation rates and increased bone resorption and osteoclast numbers acutely after injury [26]

43. Subchondral bone thinning and volumetric loss is observed within first 2 weeks of injury, recovering up to 4 weeks post-injury. Subchondral bone thickening is observed during chronic disease [26, 29]

44. It is recommended to program load and displacement limits to avoid overloading or damage to load cells, fixtures, or the mechanical testing system. For rats, a load limit of 90–150N and a displacement limit of 3.5–4.5 mm is recommended. These are dependent on strain and skeletal size, and careful preliminary testing is recommended to determine these limits.

Acknowledgments

Dr. Christiansen is supported by the National Institute of Arthritis and Musculoskeletal and Skin Diseases under Award Numbers R01 AR071459, AR075013, and AR075013–02S1, and by the Department of Defense under Award Number PR180268P1. Dr. Chan is supported by the National Science Foundation (CAREER Award 1944394) and the Indiana Clinical and Translational Sciences Institute, which is funded in part by Award Number UL1TR002529 from the National Institutes of Health, National Center for Advancing Translational Sciences, Clinical and Translational Sciences Award). Dr. van der Meulen is supported by the National Institute of Arthritis and Musculoskeletal and Skin Diseases under Award Numbers R21 AR071587. R01 AR071459, AR075013, and AR075013–02S1, and by the Department of Defense under Award Number PR180268P1. Dr. Maerz is supported by the Congressionally-Directed Medical Research Program (CDMRP, Award W81XWH-15–1-0186, PI: Kevin Baker) and the Michigan Integrative Musculoskeletal Health Core Center (P30 AR069620, National Institute of Arthritis and Musculoskeletal and Skin Diseases). The content is solely the responsibility of the authors; the funding bodies were not involved with the writing of this chapter. The authors have no conflicts of interest to disclose.

References

1. Poulet B, Hamilton RW, Shefelbine S, et al. (2011) Characterising a novel and adjustable non-invasive murine knee joint loading model. Arthritis Rheum 1:137–47
2. Poulet B, Westerhof TA, Hamilton RW, et al. (2013) Spontaneous osteoarthritis in Str/ort mice is unlikely due to greater vulnerability to mechanical trauma. Osteoarthritis Cartilage 5:756–63
3. Poulet B, de Souza R, Kent AV, et al. (2015) Intermittent applied mechanical loading induces subchondral bone thickening that may be intensified locally by contiguous articular cartilage lesions. Osteoarthritis Cartilage
4. Ko FC, Dragomir C, Plumb DA, et al. (2013) In vivo cyclic compression causes cartilage degeneration and subchondral bone changes in mouse tibiae. Arthritis Rheum 6:1569–78
5. Wu P, Holguin N, Silva MJ, et al. (2014) Early response of mouse joint tissues to noninvasive knee injury suggests treatment targets. Arthritis Rheumatol
6. Christiansen BA, Anderson MJ, Lee CA, et al. (2012) Musculoskeletal changes following non-invasive knee injury using a novel mouse model of post-traumatic osteoarthritis. Osteoarthritis Cartilage 7:773–82
7. Lockwood KA, Chu BT, Anderson MJ, et al. (2014) Comparison of loading rate-dependent injury modes in a murine model of post-traumatic osteoarthritis. J Orthop Res 1:79–88
8. Onur TS, Wu R, Chu S, et al. (2014) Joint instability and cartilage compression in a mouse model of posttraumatic osteoarthritis. J Orthop Res 2:318–23
9. Rai MF, Duan X, Quirk JD, et al. (2017) Post-Traumatic Osteoarthritis in Mice Following Mechanical Injury to the Synovial Joint. Sci Rep:45223 [PubMed: 28345597]
10. Blaker CL, Little CB, Clarke EC (2017) Joint loads resulting in ACL rupture: Effects of age, sex, and body mass on injury load and mode of failure in a mouse model. J Orthop Res 8:1754–63
11. Maerz T, Kurdziel MD, Davidson AA, et al. (2015) Biomechanical Characterization of a Model of Noninvasive, Traumatic Anterior Cruciate Ligament Injury in the Rat. Ann Biomed Eng 10:2467–76
12. Ramme AJ, Lendhey M, Raya JG, et al. (2016) A novel rat model for subchondral microdamage in acute knee injury: a potential mechanism in post-traumatic osteoarthritis. Osteoarthritis Cartilage 10:1776–85
13. Ramme AJ, Lendhey MS, Strauss EJ, et al. (2018) A Biomechanical Study of Two Distinct Methods of Anterior Cruciate Ligament Rupture, and a Novel Surgical Reconstruction Technique, in a Small Animal Model of Posttraumatic Osteoarthritis. J Knee Surg 1:43–9
14. Brown SB, Hornyak JA, Jungels RR, et al. (2019) Characterization of Post-Traumatic Osteoarthritis in Rats Following Anterior Cruciate Ligament Rupture by Non-Invasive Knee Injury (NIKI). J Orthop Res
15. Lepley LK, Davi SM, Butterfield TA, et al. Visualization of Knee Joint Degeneration after Non-invasive ACL Injury in Rats. Cambridge, MA: JoVE; 2020.
16. Hsia AW, Tarke FD, Shelton TJ, et al. (2018) Comparison of knee injury threshold during tibial compression based on limb orientation in mice. J Biomech

17. Lynch ME, Main RP, Xu Q, et al. (2010) Cancellous bone adaptation to tibial compression is not sex dependent in growing mice. J Appl Physiol 3:685–91
18. Holguin N, Brodt MD, Sanchez ME, et al. (2013) Adaptation of tibial structure and strength to axial compression depends on loading history in both C57BL/6 and BALB/c mice. Calcif Tissue Int 3:211–21
19. Ko FC, Dragomir CL, Plumb DA, et al. (2016) Progressive cell-mediated changes in articular cartilage and bone in mice are initiated by a single session of controlled cyclic compressive loading. J Orthop Res 11:1941–9
20. Adebayo OO, Ko FC, Goldring SR, et al. (2017) Kinematics of meniscal- and ACL-transected mouse knees during controlled tibial compressive loading captured using roentgen stereophotogrammetry. J Orthop Res 2:353–60
21. Sebastian A, Murugesh DK, Mendez ME, et al. (2020) Global Gene Expression Analysis Identifies Age-Related Differences in Knee Joint Transcriptome during the Development of Post-Traumatic Osteoarthritis in Mice. Int J Mol Sci 1
22. Satkunananthan PB, Anderson MJ, De Jesus NM, et al. (2014) In vivo fluorescence reflectance imaging of protease activity in a mouse model of post-traumatic osteoarthritis. Osteoarthritis Cartilage 10:1461–9
23. Gilbert SJ, Bonnet CS, Stadnik P, et al. (2018) Inflammatory and degenerative phases resulting from anterior cruciate rupture in a non-invasive murine model of post-traumatic osteoarthritis. J Orthop Res
24. Hsia AW, Anderson MJ, Heffner MA, et al. (2017) Osteophyte formation after ACL rupture in mice is associated with joint restabilization and loss of range of motion. J Orthop Res 3:466–73
25. Anderson MJ, Diko S, Baehr LM, et al. (2016) Contribution of mechanical unloading to trabecular bone loss following non-invasive knee injury in mice. J Orthop Res 10:1680–7
26. Maerz T, Newton MD, Fleischer M, et al. (2020) Traumatic joint injury induces acute catabolic bone turnover concurrent with articular cartilage damage in a rat model of posttraumatic osteoarthritis. Journal of orthopaedic research
27. Maerz T, Newton MD, Kurdziel MD, et al. (2016) Articular cartilage degeneration following anterior cruciate ligament injury: a comparison of surgical transection and noninvasive rupture as preclinical models of post-traumatic osteoarthritis. Osteoarthritis Cartilage 11:1918–27
28. Maerz T, Fleischer M, Newton MD, et al. (2017) Acute mobilization and migration of bone marrow-derived stem cells following anterior cruciate ligament rupture. Osteoarthritis Cartilage 8:1335–44
29. Maerz T, Kurdziel M, Newton MD, et al. (2016) Subchondral and epiphyseal bone remodeling following surgical transection and noninvasive rupture of the anterior cruciate ligament as models of post-traumatic osteoarthritis. Osteoarthritis Cartilage 4:698–708

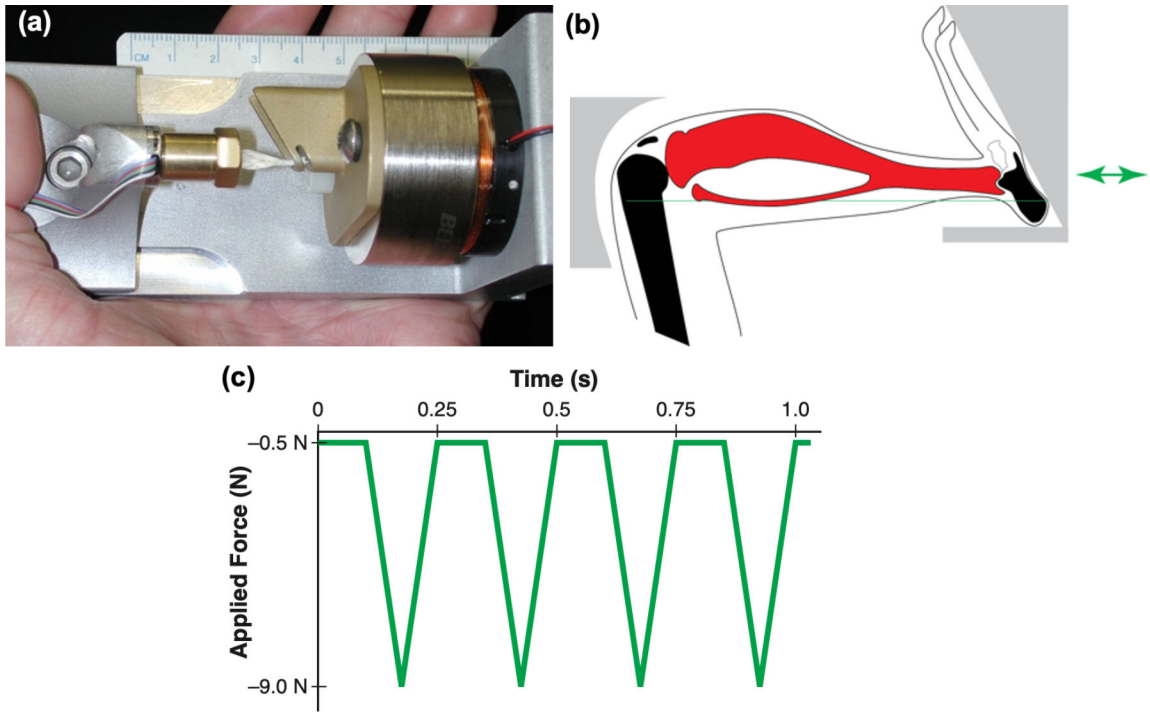

Figure 1:
(a-b): Handheld loading system used for cyclic compression loading of mice. (c): Commonly used waveform for the cyclic compression model.

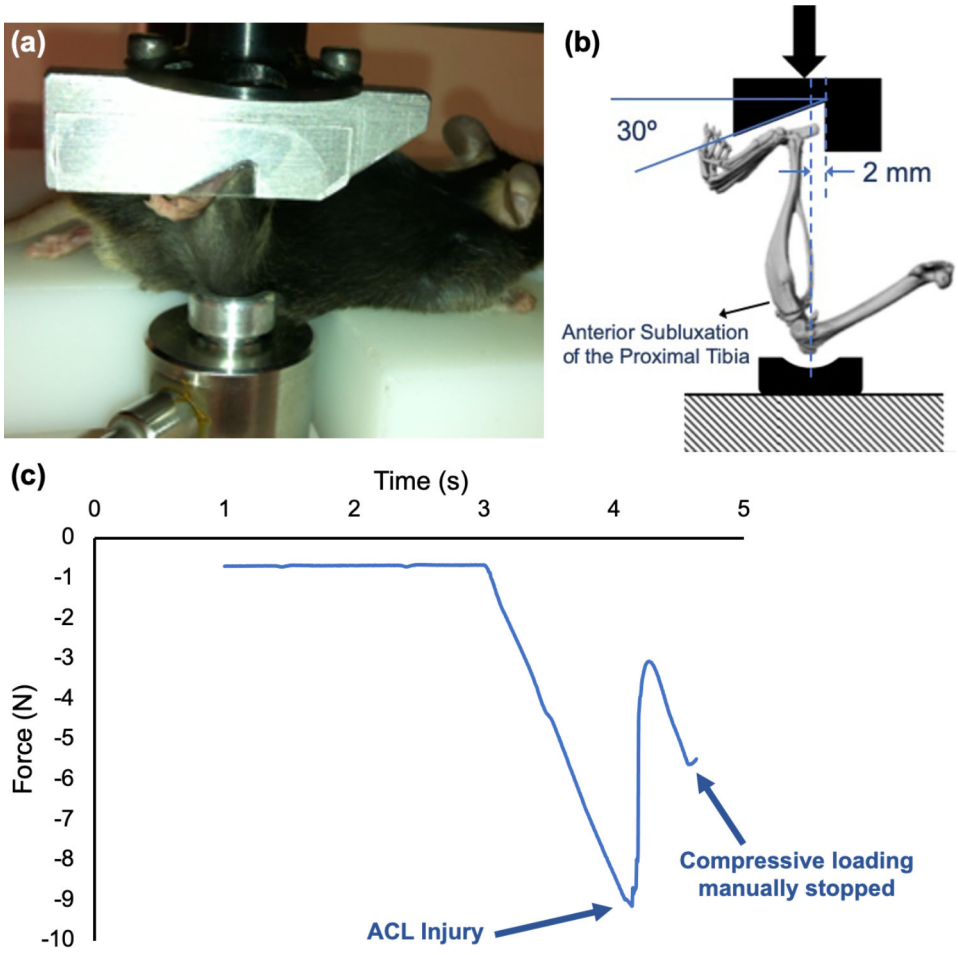

Figure 2:
(a-b): Configuration for inducing ACL-R in mice. (c): Representative compressive load that resulted in ACL rupture in a mouse knee.

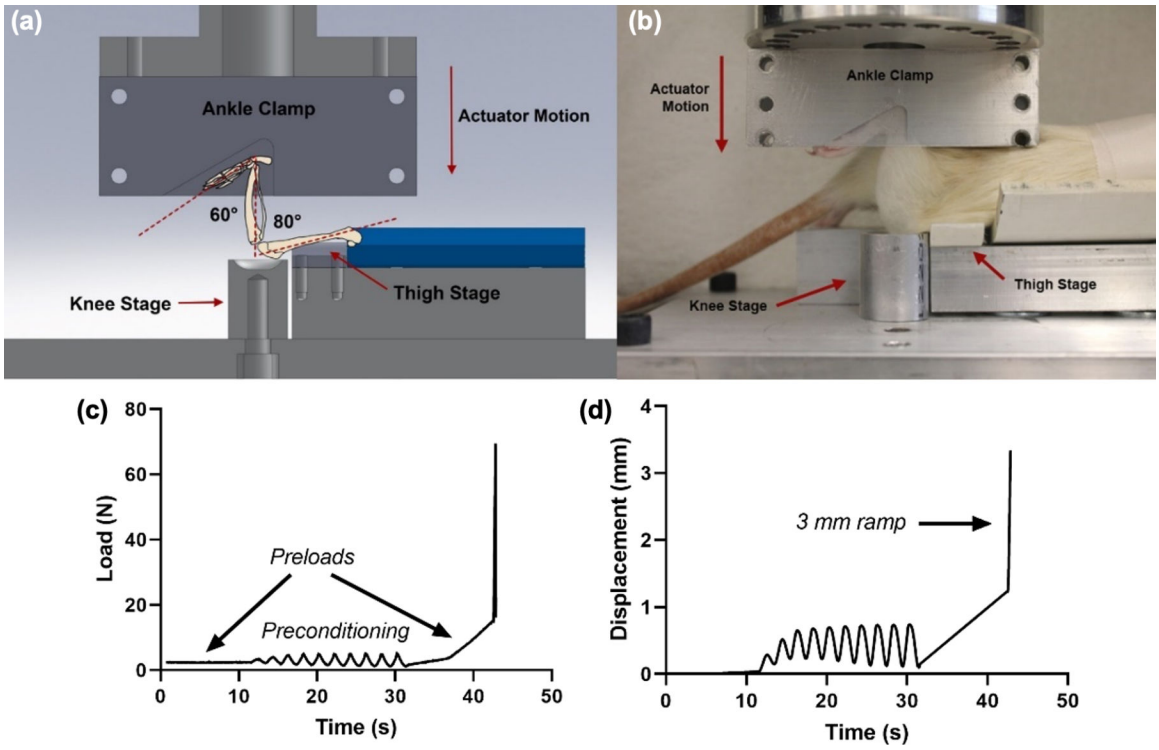

Figure 3:
(a-b): Configuration for inducing ACL-R in rats. (c-d): Load and displacement plots for preconditioning and injury load in a rat ACL-R model.